Assessment of immersion cooling fluids for electric vehicle battery thermal management

Daccord Rémi[1], Jason R. Juhasz[2]

[1] EXOES, France, remi.daccord@exoes.com

[2] CHEMOURS, United-States, jason.r.juhasz@chemours.com

Summary

State-of-the-art lithium ion batteries are powering a revolution in both emission-free transport and high-end consumer electronics, but a significant opportunity exists in the improvement of their charging time. Fast charging will change the usage of the electric vehicles by enabling several charge and discharge cycles per hour. This will lead to an increased heat load on the cells and thus require an improved cooling system design. The main focus of the paper will be on aspects of immersion cooling and the performance assessment of the dielectric fluid that comes directly into contact with the cells to remove excessive heat generated by them.

Keywords: battery, BEV (battery electric vehicle), fast charge, heat exchange, power density, thermal management

1 Introduction

The fast charging is viewed as one of the key enablers for electric vehicles (EVs) mainstream adoption [1]. New cells with higher voltage battery packs are being integrated by several of the OEMs in efforts to achieve this customer expectation. Fast charging will change the usage of the electric vehicles by enabling several charge and discharge cycles per hour. New and improved cooling systems will be required as a direct result of these increased heat loads potentially being applied during this fast recharging process. Over the last several years, dedicated projects have been initiated around this thermal management issue to provide both compact and high performing solutions [2].

Tier 1 automotive manufacturers are developing new products in battery thermal management (BTM) area ranging from forced air cooling, used in the first electric cars such as the Renault Zoé, to the immersion cooling, now used in concept cars such as the Taiwanese "Miss R" of Xing Mobility. While immersion is a new approach, working with water-glycol pumping, used in the first Tesla model S, or even refrigerant boiling in cold plates, used in the BMW i3, are being proposed. As an increased heat density removal is required for the battery thermal systems, the question is whether OEMs will converge to a single preferred solution collectively or will they operate independently with separate cooling strategy for each segment? Each of the BTM systems has both positive and negative attributes for their potential use, these pros and cons are illustrated in Table 1.

The addition of immersion as a cooling strategy appears to be the latest and most novel approach being applied yet to address this problem. And as such, there are only a limited number of projects to date actively investigating immersion on both its merits and benefits over existing alternatives. The key advantages would

make one believe that implementation could happen very soon especially in premium cars designed for fast charging and high performances. This technology adoption would then eventually trickle down to the mass EV market. Indeed, this solution has the unique capability to directly cool all the battery components, not only the cells: electrodes, bus bars, wires, electronics (balancing resistors…) etc. and does not require extra space inside the battery pack. There are no additional requirements of heat exchangers or large ducts, only inlet and outlet ports for the fluid. This will allow other BTM components to be located in more desirable locations in the car to reduce overall footprint.

Table 1: Comparison of BTM systems

	Air (forced)	Liquid Pumping (glycol and water)	Refrigerant	Immersion Cooling
Pros	- No secondary cooling loop - No liquid leak potential - Simple design - Low cost - Low maintenance	- More uniform temperature - Good heat transfer - Better thermal control - Low volume, compact	- Good heat transfer - Low volume, compact - Low system cost	- High heat transfer - Most uniform temperature across BTM - Forced convection or pooling boiling - Limits runaway potential
Cons	- Low heat transfer - More temperature variation in BTM - Heating required - Battery vent potential into cabin - Packaging of duct and fan	- Requires system integration - Potential for leak - Higher cost	- Difficult thermal control - Cooling homogeneity risk - Heating required - A/C leakage requires maintenance	- Weight of cooling liquid - Cost of dielectric fluid - Design complexity - Requires a heat sink

The performance of an immersion cooling system resides in the dielectric nature of the fluid itself, which also bears a significant portion of the complexity to the system. In accordance to the principles of thermodynamics, a strong dielectric material would mean excellent insulating properties or poor heat transfer coefficients, thus leading one at first glance be it to be a constraint to the system. But since the cells are submerged, heat is transferred directly from the cell to fluid; performance is directly dependent to the latent heat of vaporization, surface tension and densities within one caveat, that the critical heat flux is not exceeded. Both geometry of the battery cells and material compatibility are critical to the functionality of this cooling technology. New fluids are being developed for this market and this paper will disclose the test results for Opteon™ SF33 developed by the Chemours Company against a benchmark with Vertrel™ XF, existing cooling fluid in use for power electronics or electric components.

Table 1: fluid characteristics

Properties	Opteon™ SF33	Vertrel™ XF	Units
Boiling point	33.4	55	°C
Density @ 25°C	1.36	1.62	g/cm³
Heat of vaporization	169	130	kJ/kg
Liquid specific heat @ 25°C	1.20	0.77	kJ/kg/K
Dielectric strength, 0.1" gap	11.5	32	kV

Volume resistivity	5.8E8	3.8E10	Ohm.cm
Ozone depletion potential	0	0	-
Global warming potential	2	1650	-

2 Key design parameters assessment

The main objectives for this study are to increase knowledge on immersion cooling and the understanding of key fluid specifications for such an application. This applies not only for the cooling capability but for a broader perspective of the entire system level. In order to appropriately assess the system impact with the working fluid, the testing would need to be incorporated into a representative environment. But we will go for this objective step by step. A first phase will enable us to assess the key physical phenomena. A second phase will be implemented at the cell level. And then the last step concerns the system which would be a battery module, based on prismatic cells design, connected to a test rig to simulate the cooling loop that would be installed on a vehicle. This paper yields the results of the first of these steps.

2.1 A test rig for data generation

Besides the maximal temperature of a battery pack, the key performance criteria are the temperature discrepancy between minimal and maximal temperature over a cell and between cells as well as the energy consumption to effectively cool down the battery. The first indicator is linked to the proportion of the surface of cell touched by the fluid and on the heat transfer coefficient at that location, whereas the latter indicator is dictated by the flow required and the pressure drop, and above all by the thermal resistance between the ambient air and the cell surface. Immersion cooling is capable of improving most of these parameters.

A mobile test rig has been developed so that it can be placed in a climatic chamber to assess the performances of the fluids in a wide range of ambient temperatures. In this rig, the dielectric fluid is pumped through a hermetic chamber in direct contact with heating resistor and is then cooled through a radiator equipped with a fan. An expansion vessel is used in order to set the pressure in the loop to a desired value: under, above and equal to the atmospheric pressure.
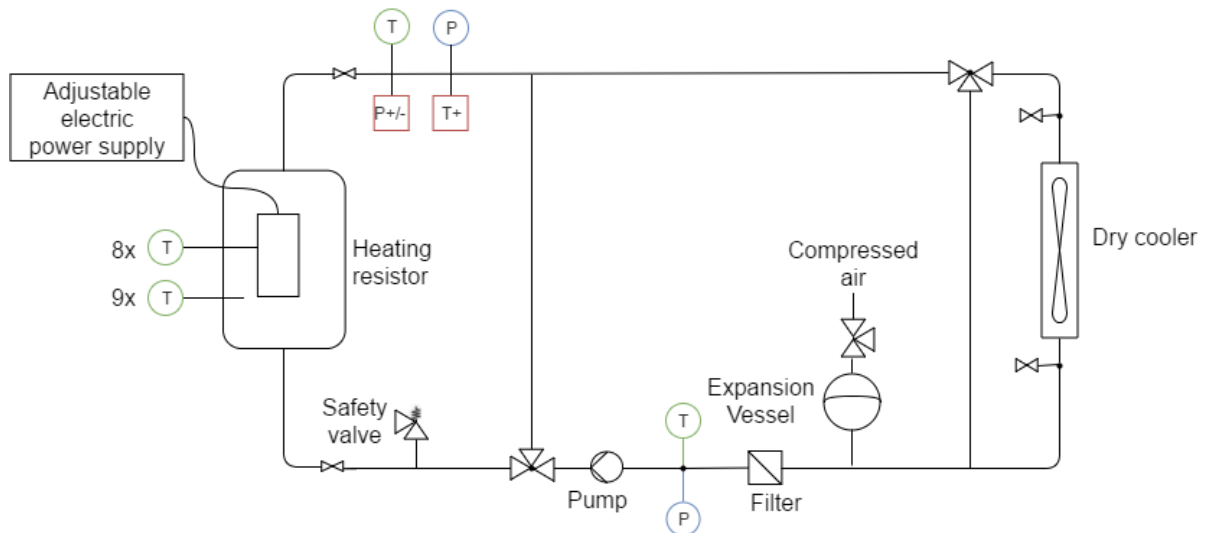

Figure 1: Test rig layout

The heating resistor can generate up to 1.2kW of heat and is encapsulated in a stainless steel sleeve displaying 41cm² of external surface. The heat flux can then approach 300kW/m², though the initial tests presented below have been done at a maximal ~150 kW/m² flux to guarantee a homogenous surface temperature. For higher fluxes, a copper sleeve could be more adapted (thermal conductivity of copper is more than 20 times higher than stainless steel).
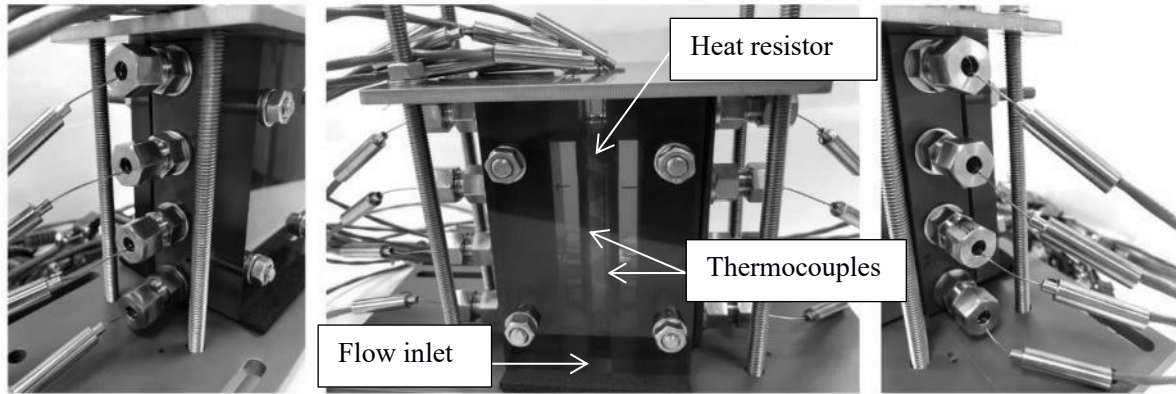
Figure 2: Instrumented heating resistor setup

2.2 Data analysis

Among the various results obtained, the focus will be on the heat transfer coefficients as compared with those found in literature [3] on different fluids. These coefficients are calculated based on the exact electric power sent to the dummy cells and their skin temperature measured in several places as show in equation (1).

$$h_{fluid} = \frac{\dot{Q}_{cell}}{S_{cell} \cdot (T_{cell} - T_{fluid})} \tag{1}$$

with h heat transfer coefficient, $\dot{Q}$ heat power, S surface and T temperature

This heat transfer coefficient largely depends on the local speed of the fluid or on the local phase of the fluid (liquid or boiling). In order to assess the upper and lower limits of the coefficient, we performed the tests in the two following conditions: a single phase static bath and a two phase pool boiling.

In addition to these results, it is fundamental to understand and to calculate the uncertainty linked to the experiment as described in equation (2).

$$\Delta h_{fluid} = h_{fluid} \cdot \left(\frac{\Delta S_{cell}}{S_{cell}} + \frac{\Delta \dot{Q}_{cell}}{\dot{Q}_{cell}} + 2. \frac{\Delta T}{(T_{cell} - T_{fluid})} \right) \tag{2}$$

with $\Delta S_{cell}, \Delta \dot{Q}_{cell}$ and ΔT representing the uncertainties on the parameters

ΔS_{cell} can be neglected as the precision of the machining is much better than any other parameters in this experiment. The control system of the heating resistor can provide the following accuracy: $\frac{\Delta \dot{Q}_{cell}}{\dot{Q}_{cell}} = \pm 2\%$. Regarding the last expression in the equation, the initial temperature sensors and acquisition line were sensitive enough and resulted in the typical ΔT amounts to $\pm 1K$. This increased the uncertainty to 20% and 200% when the temperature spread between fluid and wall is respectively close to 10K and 1K which is likely to occur at small power and evaporative conditions. This effect is shown in the error bars in the graph below. In parallel, a complete calibration of the temperature acquisition has been launched with the target to reduce the uncertainty to $\pm 0.1K$.

2.3 Initial test results

The first set of results is shown below with the two previously mentioned fluids: Opteon™ SF33 and Vertrel™ XF. The two different cooling modes, liquid and evaporative, are easily distinguishable from one another. The tests are performed with no flow, so that only natural convection occurs. In single phase static bath, the coefficient average 240 ± 60 W/m²/K whereas in 2-phase evaporative pool, the SF33 shows up to 2800 ± 6400 W/m²/K. Though the results are encouraging, the measurement uncertainty is preposterously high. This compelled us to revise the temperature acquisition line. But the interesting point is that the wall superheating is reduced by a factor of 5 to 10. From the application point of view, this fact reduces the effort (and the energy consumption) of the cooling system to effectively keep the battery cells under a temperature threshold (typ. 50°C).
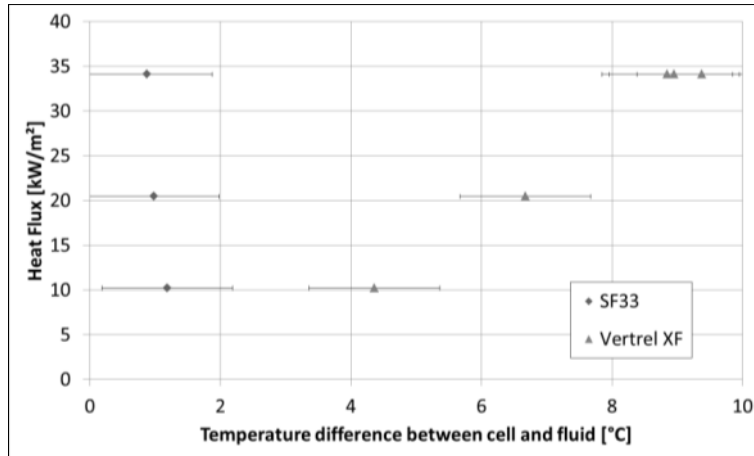
Figure 3: Heat fluxes versus temperature difference for two fluids

Further tests have been pursued on Opteon™ SF33: they are detailed below. At first, we controlled the system to test different subcooling conditions of the fluid at the setup inlet in order to assess its impact. The flow was kept constant during the test, around 1.5 L/min which gives an average 0.05 m/s fluid speed around the heat resistor. The tests (Figure 4) clearly demonstrated that what has to be considered is the temperature gap to the fluid saturation temperature. When the wall temperature gets closer or even overpass the saturation temperature the heat transfer rate increases suddenly. Up to 8K below the saturation, the fluid shows steady behavior with a constant heat transfer rate around 660 W/m²/K whatever the subcooling conditions at fluid inlet. Above -8K, the behavior changes and heat transfer rises as evaporation begins.

The temperature saturation calculation is based on the pressure measurement and a theoretical calculation based on a Refprop file. In addition, some air may be trapped in the system that adds an air partial pressure. Both phenomena lead to a potential shift in the saturation temperature calculation. The following results have to be considered with this in mind. These 8K are difficult to explain, except by the presence of air in the system that flaws the saturation temperature calculation. One would have expected a value closed to 0K and 400mbar of air partial pressure is sufficient to explain an 8K shift.
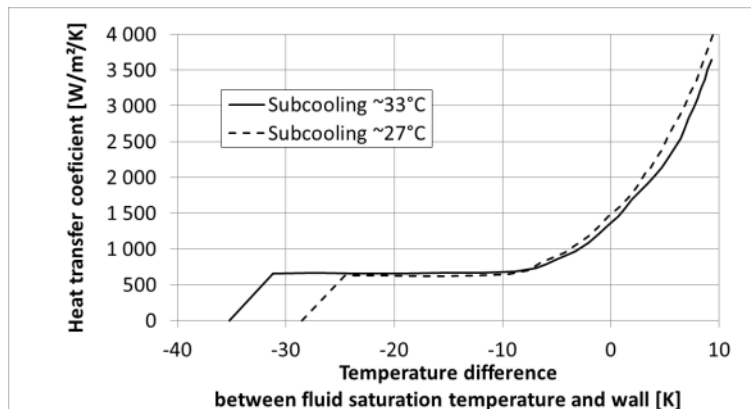

Figure 4: Fluid subcooling impact on the heat transfer rate for SF33

As a consequence, the following results will only be presented as the difference between the wall to the fluid saturation temperatures. In the following graphs (Figures 5 and 6), a better fluid filling process has been implemented and little air was trapped: the position of the change in thermal behavior is closer to the saturation. In Figure 5, the heat flux has been raised up to 40 kW/m². We can observe a clear change in the thermal properties at 1K to the saturation when the evaporation occurs enabling to transfer higher power without increasing the wall temperature.
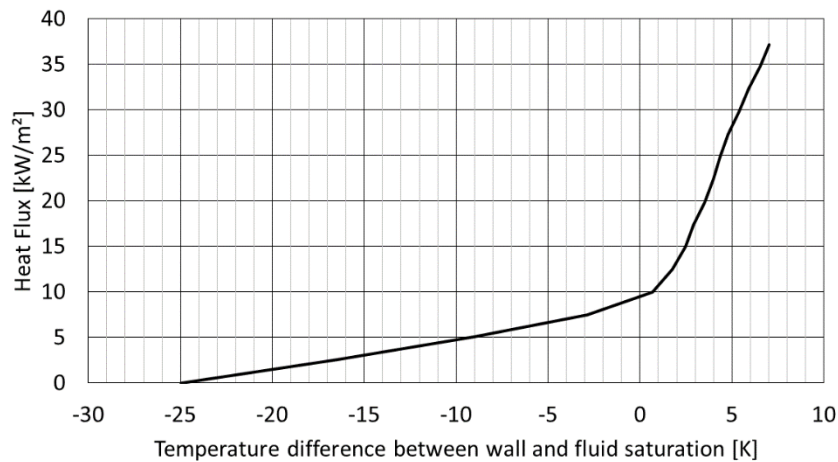
Figure 5: Heat fluxes for SF33 according to the wall superheating

The heat transfer coefficient calculated is lower than in Figure 4. The fluid velocity around the heating resistor was reduced to 0.01 m/s.
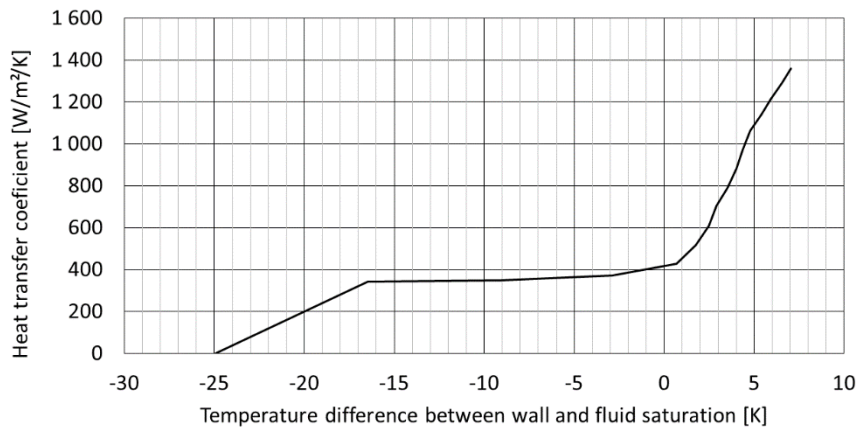

Figure 6: Heat transfer rate for SF33 according to the wall superheating

As a conclusion, for a use in a battery cooling application which typically a maximal average heat flux under 40 kW/m², we can imagine a cooling system with a performance of more than 350 - 750 W/m²/K in liquid cooling with SF33 (according to the local fluid speed). And locally, on hot spots, the fluid may evaporates providing much higher heat transfer capacity that will instantaneously cool down the hot spots. It seems to be a self-adaptive cooling system always keeping the battery on the safe side. Even a thermal runaway event could be contained and its propagation avoided. Further tests and simulation have to be performed to demonstrate it.

3 Simulation at the cell level

Cell simulations up to 10Crms were conducted and this allowed for cell temperature assessment.

3.1 3D orthotropic modelling

The battery cell model was built under LISA, a readily available finite element analysis software, as if the cell was a homogenous material with anisotropic thermal properties. A prismatic cell has a lower conductive

thermal coefficient in the direction normal to the electrode plane than in-plane. On top of this, we add an aluminium casing all around it that has a great impact on the temperature gradient.

This material receives also a homogenous heating energy directly linked to the volumetric energy generated by Joule effect due to the cell internal resistance. The amount of energy generated stands for a C-rate of 10 for a high power type cell or for a typical fast charge profile with a high energy type cell.

A pre-selected constant for the heat transfer rate was chosen on each surface to simulate an immersive behaviour except on the large lateral surfaces. On these surfaces, we simulated a heat flux equals to zero for design reasons: we intend to package the cells squeezed against each other.

Table 2: simulation parameters

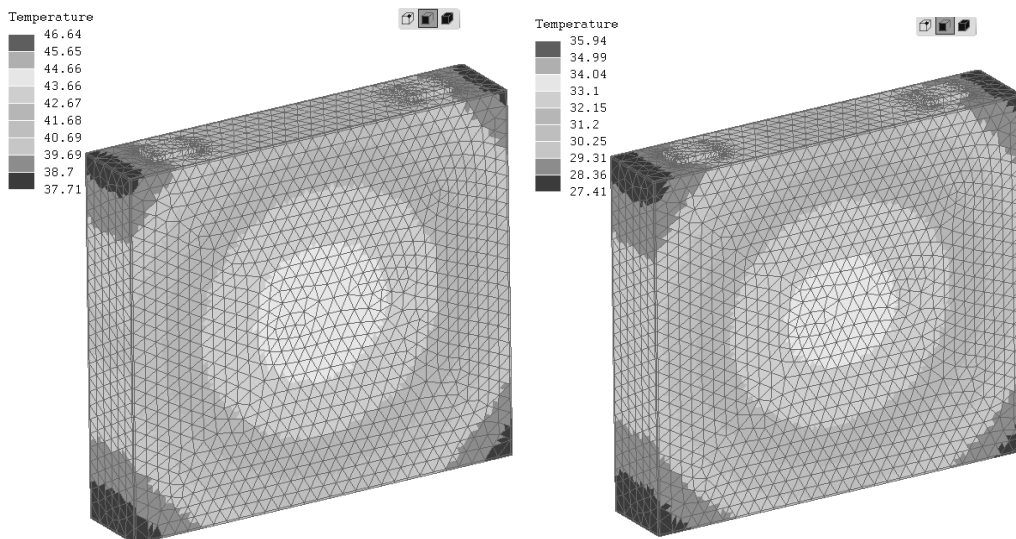| Parameter	Value	Unit
Normal conductive coefficient	0.8	W/m/K
In-plane conductive coefficient	35	W/m/K
Aluminum conductive coefficient	220	W/m/K
Aluminum casing thickness	0.5	mm
Convective coefficient	350 or 750	W/m²/K
Heating power	265	kW/m^3

3.2 Simulation results

Figure 7: 3D stationary thermal simulation
with 350W/m²/K on the left picture and 750 W/m²/K on the right picture
these coefficients are applied only on the 4 small surfaces. The 2 large surfaces are considered insulated
the fluid temperature is set at 20°C

The results are summed up in the table 3 and illustrate the mere fact that it is possible to design a cooling system which guarantees a temperature spread less than 10°C with passive solutions (only natural convection or pool boiling evaluated here). The high heat transfer rate enables one to alleviate the load on the cooling system by reducing the thermal resistance between the cell and the ambient air, but it has little impact on the temperature spread across the cell itself. We can already conclude that an immersion cooling system has to

be carefully implemented: it is not enough to flood a battery pack with a liquid to reach a perfect homogenous temperature gradient.

This simulation overly simplifies the system to some degree, and the limitations are stated as such. The internal geometry is not modelled and the electrodes are not being monitored. As a consequence overall hot spots are not modelled, potentially yielding an increase of the temperature difference.

Table 3: simulation results

Parameter	Liquid	Evaporative	Unit
Convective coefficient	350	750	W/m²/K
Maximal Temperature difference of the cell skin to the fluid	+24	+13	°C
Maximal temperature difference on the cell skin	6	5	°C
Maximal temperature difference in the cell core	9	9	°C

Moreover, a cell core temperature can be simulated. This temperature, that cannot be measured, is critical for high power applications. Indeed, a strong internal gradient can appear due to both a strong core heating and a strong skin cooling thanks to immersion. This core temperature triggers the degradation of the cell; typically above 80°C the internal separator begins its degradation. It is then possible to simulate use profiles of the cell off-line in order to assess a new criterion to avoid the cell degradation.

4   Future tests on a representative module

Regarding the battery module, an intermediate approach between testing a unitary cell and testing a complete large battery pack was applied. Thermal behaviours are largely dependent of the scale at which they are studied. Testing a representative sub-assembly of a complete pack was then required and a module with 36 prismatic cells was constructed. It includes a battery management system on an electronic board also immersed in the fluid.

Figure 8: Battery module equipped with prismatic dummy cells

As a first step, the cells will be replaced by dummy cells that enclosed heat resistors. This will allow for a representative thermal behaviour without incurring potential safety issues with the use of lithium cells. The heat resistors are supplied with a controlled power supply with adjustable voltage. The module is equipped with an inlet and an outlet port to circulate the liquid. Hermetic connectors are used for the electric power connection as well as for the numerous temperature sensors.

5 Conclusion

The results obtained are critical to proportion the right cooling system to the right application. Some niche markets will definitely require high performing BTM such as immersion cooling regardless of potential challenges: sealed pack, extra weight and cost of the fluid, but its unique advantages: pack compactness, improved safety and lifetime may also be the benefits for implementing in mainstream products.

New fluids, which are designed on purpose for this application, are appearing on the market giving immersion cooling a better performance, or at least reducing its drawbacks. An experimental approach was setup at the battery module level in order to assess the performance of a new high promising dielectric liquid. Coupled to a simple simulation tool, we were able to pre-size a cooling system that would allow 5 K temperature difference on the cell surfaces of a battery pack.

Our next steps are to continue in these developments toward a proof of concept of a battery pack able to ultra-fast charge without showing a temperature discrepancy above ± 1K. The simulation model will be improved taking into account the effective internal geometry and it will be calibrated on tests results.

References

[1] Wandt et al, *Quantitative and time-resolved detection of lithium plating on graphite anodes in lithium ion batteries*, Materials Today, volume 21, issue 10 (December, 2017) http://dx.doi.org/10.1016/j.mattod.2017.11.001

[2] Matthew Keyser et al., *Enabling fast charging – Battery thermal considerations*, Journal of Power Sources, Volume 367, 1 November 2017, Pages 228-236 https://doi.org/10.1016/j.jpowsour.2017.07.009

[3] van Gils, Rob & Danilov, Dmitry & Notten, Peter & Speetjens, Michel & Nijmeijer, Henk. (2014). *Battery thermal management by boiling heat-transfer*. Energy Conversion and Management. 79. 9–17. 10.1016/j.enconman.2013.12.006.

Authors

Rémi DACCORD, EXOES, CTO, CIPO & founder (2009). He leads the technical development in automotive bottoming Rankine cycles or in battery thermal management. Rémi has applied for more than 20 patents since 2009. Former to EXOES, he created AMOES in 2007, an engineering company dedicated to designing low consumption buildings using micro combined heat to power technologies. Rémi is an engineer graduated from University "Centrale Paris" in applied physics in 2006. He is a serial entrepreneur devoted to reduce the carbon footprint of our society.

Jason R. Juhasz, Chemours, Technology Leader for Thermal Management. Previous experience in leading Process Development and Research activities in both Semiconductor and Chemical Manufacturing industries. For the last 13 years, he has been working with Fluorochemical Division with the main focus in developing the next generation HFOs as sustainable products for the environment. He has a B.S. degree in Chemistry and Chemical Engineering from the University of Florida.